Power System Technology
ISSN:1000-3673

Received: 1610-2024 Revised: 05-11-2024 Accepted: 22-12-2024

Radiation Effects on Unsteady Mhd Convective Flow of An Incompressible Viscous Fluid Via an Impulsively Initiated Vertical Plate through Porous Medium

[1]B. Lakshmanna, [2]B. Chandra Sekhar, [3]T. Mohan Reddy

[*1]Assistant Professor, Department of Mathematics, St. Joseph's Degree College, Sunkesula Road, Kurnool, A.P-518004, Email: laxman7553@gmail.com

[2]Assistant Professor, Department of Mathematics, St. Joseph's Degree College, Sunkesula Road, Kurnool, A.P-518004, Email: chandra0025@gmail.com

[3]Assistant Professor, Department of Mathematics, St. Joseph's Degree College, Sunkesula Road, Kurnool, A.P-518004, Email: mohanreddy.t2013@gmail.com

Abstract: -

The present study is to analysis the effects of Radiation on unsteady MHD flow in an impulsively begun vertical plate with variable heat and mass transfer through a partially packed porous medium. The plate's temperature is designed to increase linearly over time. The fluid in question is gray, non-scattering, and absorbs and emits radiation. The non-dimensional governing equations of the problem have been solved analytically by Laplace-transform method. The effects of various governing parameters on the flow variables are discussed quantitatively with the help of graphs for the flow field. The values of skin friction, Nusselt number and Sherwood number are determined and computationally discussed.

Keywords*:* Radiation effects, MHD flows, Heat and mass transfer, vertical plates, porous medium, Skin friction, Nusselt number, Sherwood number.

1. Introduction

The study of the oscillatory flow of an electrically conducting fluid through a porous channel saturated with porous material is significant in many physiological flows and engineering applications, including magneto-hydrodynamic (MHD) generators, arterial blood flow, petroleum engineering, and many more. Several researchers have investigated the flow and heat transmission in oscillatory fluid problems. To name a few, Makinde and Mhone [1] studied the forced convective MHD oscillatory fluid flow in a channel filled with porous media, and their calculations were based on the assumption that the plates were impervious. In a comparable work, Mehmood and Ali [2] looked at how slip affected free convective oscillatory flow over a vertical channel with periodic temperature and dissipative heat.

Power System Technology
ISSN:1000-3673

Received: 1610-2024 Revised: 05-11-2024 Accepted: 22-12-2024

In addition, Chauchan and Kumar [3] investigated the steady flow and heat transmission in a composite vertical channel. Palani and Abbas [4] used the Rosseland approximation to explore the combined effects of magnetohydrodynamics and radiation on free convection flow past an impulsively begun isothermal vertical plate. Hussain et al. [5] offered an analytical investigation of oscillatory second-grade fluid flow in the presence of a transverse magnetic field, among other topics. Several researchers have been conducted on convective heat transfer across porous channels; for example, Umavathi et al. [6] evaluated the unsteady flow of viscous fluid through a horizontal composite channel filled with porous media for half of its width. Adesanya and Makinde [7] studied the influence of radiative heat transfer on pulsatile couple stress fluid flow on a heated plate with a time-dependent boundary condition. The no-slip requirement is well understood to be unrealistic in some flows including nanochannels, microchannels, and flows across hydrophobic-coated plates. In light of this, Adesanya and Gbadeyan [8] investigated the flow and heat transfer of steady non-Newtonian fluid flow while accounting for fluid slide in the porous channel. Other fascinating examples of hydromagnetic oscillatory fluid flow under various geometries can be found in [9-16]. Seth GS et al. [17] illustrate how hall current, radiation, and rotation affect natural convection heat and mass transfer flow past a moving vertical plate. Biswas and S.F. Ahmmed [18,19] explored the effects of radiation and chemical reactions on MHD unsteady heat and mass transfer in Casson fluid as well as nanofluid flow via a vertical plate, and R. Chamkha and Khaled [20] studied the problem of coupled heat and mass transfer from an inclined plate using magnetohydrodynamics (MHD) free convection in the presence of internal heat generation or absorption. Effects of radiation and magnetic field on the mixed convection stagnation-point flow over a vertical stretching sheet in a porous medium has been investigated by Hayat at al. [21]. Sweta Matta1 at al. [22] analyzed the Radiation and chemical reaction effects on unsteady MHD free convention mass transfer fluid flow in a porous plate

Motivated by the above studies, a purpose has been carried out to study the effects of Radiation on MHD flow via an impulsively initiated vertical plate with variable heat and mass transfer have been examined in this article. Tables and graphs are used to display the results.

2. Formulation and solution of the problem

We investigate the flow of an unstable viscous incompressible fluid through a porous media and past a vertical plate. The x-axis runs vertically along the plate, whereas the y-axis runs normal to it. Initially, the fluid and plate have the same temperature. Figure 1 depicts a transverse magnetic field B0 of uniform strength applied normal to the plate. Because of their

Power System Technology
ISSN:1000-3673

Received: 1610-2024 Revised: 05-11-2024 Accepted: 22-12-2024

minor impact, viscous dissipation and induced magnetic field have been ignored. The fluid and plate are initially at the same temperature (T1) and concentration (C1) in the stationary condition. At time t > 0, the plate moves with a velocity u = u0 in its own plane, and the temperature of the plate rises to Tw, while the concentration level around the plate rises linearly with time.

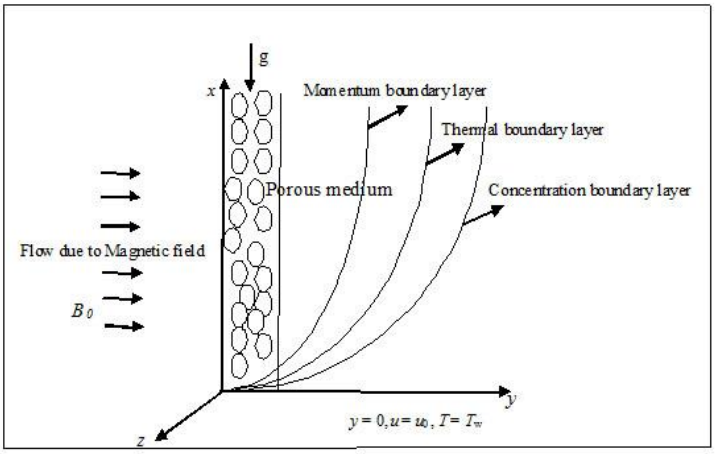

Figure 1: Physical model of the problem

The unsteady hydro magnetic equations of the MHD flow through porous medium are as:

$$\frac{\partial u}{\partial t} = \nu \frac{\partial^2 u}{\partial y^2} - \frac{\sigma_e B_0^2}{\rho} u - \frac{\nu}{K} u + g\beta(T - T_\infty) + g\beta^*(C - C_\infty) \quad (1)$$

$$\rho C_p \frac{\partial T}{\partial t} = k \frac{\partial^2 T}{\partial y^2} - \frac{\partial q_r}{\partial y} \quad (2)$$

$$\frac{\partial C}{\partial t} = D_1 \frac{\partial^2 C}{\partial y^2} \quad (3)$$

The initial and boundary conditions

$$u = 0, T = T_\infty, C = C_\infty, \quad t \le 0, \ \forall \ y \quad (4)$$

$$u = u_0, T = T_\infty + (T_w - T_\infty)At, C = C_\infty + (C_w - C_\infty)At, \quad y = 0 \quad (5)$$

$$u \to 0, T \to T_\infty, C \to C_\infty, \quad y \to \infty \quad (6)$$

Where $A = \frac{u_0^2}{\nu}$,

Power System Technology
ISSN:1000-3673

Received: 1610-2024 Revised: 05-11-2024 Accepted: 22-12-2024

The local radiant for the case of an optically thin gray gas is expressed by

$$\frac{\partial q_r}{\partial y} = -4a^*\sigma(T_\infty^4 - T^4) \tag{7}$$

Considering the temperature difference within the flow sufficiently small, T^4 can be expressed as the linear function of temperature. This is accomplished by expanding T^4 in a Taylor series about T_∞ and neglecting higher-order terms, thus

$$T^4 \cong 4T_\infty^3 T - 3T_\infty^4 \tag{8}$$

Using equations (7) and (8), equation (2) reduces to

$$\rho C_p \frac{\partial T}{\partial t} = k\frac{\partial^2 T}{\partial y^2} + 16a^*\sigma(T_\infty^3 - T^4) \tag{9}$$

Introducing the following non- dimensional quantities:

$$u^* = \frac{u}{u_0}, y^* = \frac{yu_0}{\nu}, \theta = \frac{T - T_\infty}{T_w - T_\infty}, C^* = \frac{C - C_\infty}{C_w - C_\infty}, \mu = \rho\nu, t^* = \frac{tu_0^2}{\nu}$$

Making use of non-dimensional variables, the equations (1), (2) and (9) leads to (dropping asterisks)

$$\frac{\partial u}{\partial t} = \frac{\partial^2 u}{\partial y^2} - \left(M^2 + \frac{1}{D}\right)u + Gr\,\theta + Gm\,C \tag{10}$$

$$\frac{\partial \theta}{\partial t} = \frac{1}{P_r}\frac{\partial^2 \theta}{\partial y^2} - \frac{R}{P_r}\theta \tag{11}$$

$$\frac{\partial C}{\partial t} = \frac{1}{Sc}\frac{\partial^2 C}{\partial y^2} \tag{12}$$

With boundary conditions

$$u = 0, \theta = 0, C = 0, \quad t \le 0, \ \forall\ y \tag{13}$$

$$u = 1, \theta = t, C = t, \quad y = 0 \tag{14}$$

$$u \to 0, \theta \to 0, C \to 0, \ as \ \ y \to \infty \tag{15}$$

Where, $R = \frac{16a^*\nu^2\sigma T_\infty^3}{ku_0^2}$ is the Radiation parameter, $M^2 = \frac{\sigma_e B_0^2 \nu}{\rho u_0^2}$ is the Hartmann number, $D = \frac{ku_0^2}{\nu^2}$

Power System Technology
ISSN:1000-3673

Received: 1610-2024 Revised: 05-11-2024 Accepted: 22-12-2024

is the Darcy parameter, $Gr = \frac{g\beta\nu(T_w - T_\infty)}{u_0^3}$ is the thermal Grashof number, $Gm = \frac{g\beta^*\nu(C_w - C_\infty)}{u_0^3}$ the mass Grashof number, $\Pr = \frac{\mu C_p}{k}$ is Prandtl parameter and $Sc = \frac{\nu}{D_1}$ is the Schmidt number.

The dimensionless governing equations (10) to (12), subject to the boundary conditions (13) to (15), are solved by the usual Laplace transform technique. With help of Hetnarski's (1975) development has also been taken. The solutions derived are given below. Transforming equation (12) we get,

$$s\bar{C}(y,s) - C(y,0) = \frac{1}{Sc}\frac{d^2\bar{C}}{dy^2} \tag{16}$$

Using boundary conditions (13) to (15), we have,

$$\frac{d^2\bar{C}}{dy^2} - s\,Sc\,\bar{C}(y,s) = 0 \tag{17}$$

The solution of the equation (16) is

$$\bar{C}(y,s) = Ae^{\sqrt{sSc}y} + Be^{-\sqrt{sSc}y} \tag{18}$$

Where *A* and *B* are arbitrary constants.

Again, using above boundary conditions (13) and (14), we get,

$$\bar{C}(y,s) = \frac{1}{s^2}e^{-\sqrt{sSc}y} \tag{19}$$

Taking inverse Laplace transform for the equation (19) from Campbell and Foster (1948) and Spiegel.M.R.(1986), we obtained

$$C(y,t) = t\left(1 + 2\left(\frac{y}{2\sqrt{t}}\right)^2 Sc\right)erfc\left(\left(\frac{y}{2\sqrt{t}}\right)\sqrt{Sc}\right) - \frac{2\left(\frac{y}{2\sqrt{t}}\right)\sqrt{Sc}}{\sqrt{\pi}}\,e^{-\left(\frac{y}{2\sqrt{t}}\right)^2 Sc} \tag{20}$$

Also transforming equation (11);

$$s\bar{\theta}(y,s) - \theta(y,0) = \frac{1}{\Pr}\frac{d^2\bar{\theta}}{dy^2} - \frac{R}{\Pr}\bar{\theta}(y,s) \tag{21}$$

Using boundary conditions (13) and (14), it reduces to:

$$\frac{d^2\bar{\theta}}{dy^2} - (R + s\Pr)\bar{\theta}(y,s) = 0$$

Power System Technology
ISSN:1000-3673

Received: 1610-2024 Revised: 05-11-2024 Accepted: 22-12-2024

(22)

The solution of this equation (21)

$$\bar{\theta}(y,s) = Ce^{y\sqrt{R+s\,\mathrm{Pr}}} + Ee^{-y\sqrt{R+s\,\mathrm{Pr}}} \tag{23}$$

Where, C and E are arbitrary constants. Values of C and E can be computed using (13) and (14), we obtain

$$\bar{\theta}(y,s) = \frac{1}{s^2} e^{-y\sqrt{\mathrm{Pr}\left(s+\frac{R}{\mathrm{Pr}}\right)}} \tag{24}$$

Taking inverse Laplace transform for the equation (23), we obtain

$$\theta(y,t) = \frac{t}{2}\left(a_1 e^{2\xi\sqrt{Rt}}\, erfc(\xi\sqrt{Pr} + \sqrt{ct}) + a_2 e^{-2\xi\sqrt{Rt}}\, erfc(\xi\sqrt{Pr} - \sqrt{ct})\right) \tag{25}$$

Similarly, again taking the Laplace transform to the equation (10) and making use of the initial and boundary conditions (13) to (15), it reduces to

$$\frac{d^2\bar{u}}{dy^2} - \left[s + \left(M^2 + \frac{1}{D}\right)\right]\bar{u}(y,s) = -GrL\{\theta(y,t)\} - GmL\{C(y,t)\} \tag{26}$$

The solution of the equation (26) is

$$\bar{u}(y,s) = Fe^{y\sqrt{s+\left(M^2+\frac{1}{D}\right)}} + Ge^{-y\sqrt{s+\left(M^2+\frac{1}{D}\right)}} + \frac{Gr}{1-Pr}\frac{e^{-y\sqrt{Pr}\sqrt{s+\frac{R}{Pr}}}}{s^2(s-a_3)} + \frac{Gm}{1-Sc}\frac{e^{-y\sqrt{sSc}}}{s^2(s-a_4)} \tag{27}$$

Applying the boundary conditions (13) and (14) for (26), we obtain

$$\bar{u}(y,s) = \frac{1}{s}e^{-y\sqrt{s+\left(M^2+\frac{1}{D}\right)}} + \frac{Gr}{1-Pr}\left(\frac{e^{-y\sqrt{Pr}\sqrt{s+\frac{R}{Pr}}} - e^{-y\sqrt{s+\left(M^2+\frac{1}{D}\right)}}}{s^2(s-a_3)}\right) + \frac{Gm}{1-Sc}\left(\frac{e^{-y\sqrt{sSc}} - e^{-y\sqrt{s+\left(M^2+\frac{1}{D}\right)}}}{s^2(s-a_4)}\right) \tag{28}$$

Taking the inverse Laplace transform to the equation (28), we obtain the velocity as

$$u(y,t) = a_5\, e^{-y\sqrt{\left(M^2+\frac{1}{D}\right)}}\, erfc\left(\xi - \sqrt{\left(M^2+\frac{1}{D}\right)t}\right) + a_6\, e^{y\sqrt{\left(M^2+\frac{1}{D}\right)}}\, erfc\left(\xi + \sqrt{\left(M^2+\frac{1}{D}\right)t}\right) +$$

$$-\left[e^{-y\sqrt{\mathrm{Pr}(a_3+(R/\mathrm{Pr}))}}\, erfc(\xi\sqrt{\mathrm{Pr}} - \sqrt{(a_3+(R/\mathrm{Pr}))t}) + e^{y\sqrt{Pr(a_3+(R/Pr))}}\, erfc(\xi\sqrt{Pr} + \sqrt{(a_3+(R/Pr))t})\right]\frac{a_{11}}{2}e^{a_3 t}$$

Power System Technology
ISSN:1000-3673

Received: 1610-2024 Revised: 05-11-2024 Accepted: 22-12-2024

$$-\left(a_7\, e^{-y\sqrt{\Pr(R/\Pr)}}\ erfc\left(\xi\sqrt{\Pr}-\sqrt{(R/\Pr)t}\right)+\ a_8\, e^{y\sqrt{\Pr(R/\Pr)}}\ erfc\left(\xi\sqrt{\Pr}+\sqrt{(R/\Pr)t}\right)\right)$$

$$-\left[e^{-y\sqrt{Pr\left(M^2+\frac{1}{D}+a_3\right)}}\ erfc\left(\xi\sqrt{Pr}-\sqrt{Pr\left(M^2+\frac{1}{D}+a_3\right)t}\right)+\right.$$

$$\left.e^{y\sqrt{Pr\left(M^2+\frac{1}{D}+a_3\right)}}\ erfc\left(\xi\sqrt{Pr}+\sqrt{Pr\left(M^2+\frac{1}{D}+a_3\right)t}\right)\right]\ \frac{a_{11}}{2}e^{a_3 t}$$

$$+\left[e^{-y\sqrt{a_4 Sc}}\ erfc(\xi\sqrt{Sc}-\sqrt{a_4 t})+e^{y\sqrt{a_4 Sc}}\ erfc(\xi\sqrt{Sc}+\sqrt{a_4 t})\right]\frac{a_{12}}{2}e^{a_4 t}$$

$$-\left[e^{-y\sqrt{\left(M^2+\frac{1}{D}+a_4\right)}}\ erfc\left(\xi-\sqrt{\left(M^2+\frac{1}{D}+a_4\right)t}\right)+\ e^{y\sqrt{\left(M^2+\frac{1}{D}+a_4\right)}}\ erfc\left(\xi+\sqrt{\left(M^2+\frac{1}{D}+a_4\right)t}\right)\right]\ \frac{a_{12}}{2}e^{a_4 t}$$

$$-a_{12}\left[1+a_4 t(1+2\xi^2 Sc)erfc(\xi\sqrt{Sc})+\frac{2a_4 t\xi\sqrt{Sc}}{\sqrt{\pi}}e^{-\xi^2 Sc}\right] \tag{29}$$

The non-dimensional shear stress is given by

$$\tau=-\left(\frac{du}{dy}\right)_{y=0}=-\frac{1}{2\sqrt{t}}\left(\frac{du}{d\xi}\right)_{\xi=0} \tag{30}$$

The non-dimensional Nusselt number is given by

$$Nu=-\left(\frac{d\theta}{dy}\right)_{y=0}=-\frac{1}{2\sqrt{t}}\left(\frac{d\theta}{d\xi}\right)_{\xi=0} \tag{31}$$

The non-dimensional Sherwood number is given by

$$Sh=-\left(\frac{dC}{dy}\right)_{y=0}=-\frac{1}{2\sqrt{t}}\left(\frac{dC}{d\xi}\right)_{\xi=0} \tag{32}$$

3. Results and discussions

We gave an exact analysis to study the combined effects of heat and mass transfer on the MHD flow of an incompressible viscous fluid limited by a loosely packed porous medium in an impulsively initiated vertical plate with variable heat and mass transfer. The physical behaviour of dimensionless parameters such as Hartmann number M, Darcy parameter D (permeability parameter), radiation parameter R, thermal Grashoff number Gr, mass Grashoff number Gm, Prandtl number Pr, and Schmidt

Power System Technology
ISSN:1000-3673

Received: 1610-2024 Revised: 05-11-2024 Accepted: 22-12-2024

number Sc is also discussed. Figures (2-12) exhibit the velocity, temperature, and concentration. Tables 1-3 illustrate the skin friction, Nusselt number, and Sherwood number.

The velocity, temperature, and concentration profiles for various realistic values of Prandtl number (Pr = 0.71, 0.16, and 3 for saturated liquid Freon at 273.3˚ and Pr = 7 for water) and Schmidt number (Sc = 0.2 for hydrogen). Figure (2) depicts the velocity profile for various values of M with the other parameters fixed. We discovered that as the Hartmann number M increases, the velocity falls. The introduction of a transverse magnetic field produces a resistive type of force (Lorentz force) comparable to drag force, and raising the intensity of the magnetic field causes the flow to decelerate. Figure (3) depicts the fluctuations in the permeability parameter D.

The magnitude of the velocity is shown to rise as the permeability parameter D values increase. This is because increased permeability reduces drag force, allowing the fluid to travel much more quickly. Similarly, as the radiation parameter R increased, the magnitude of the velocity u decreased consistently (figure 4). Figures 5 and 6 illustrate how velocity varies with different values of dimensionless time t and Prandtl number Pr. It has been observed that velocity increases with increasing time t. Figure (6) shows that as the Prandtl number Pr increases, the magnitude of the velocity u decreases.

Figure (7) shows that when the thermal Grashof number Gr (cooling plate) increases, the velocity drops, whereas the velocity increases sharply when the plate is heated; this rise persists away from the plate. Figure (8) shows that the amplitude of velocity increases with increasing mass Grashoff number Gm across the fluid region. Figure 9 shows the same pattern with increasing Schmidt number Sc. Figure 10 shows the effect of the radiation parameter R on the temperature profile. It has been discovered that as the temperature decreases as a function of R, the fluid flow and velocity slow down. Such an impact may also be expected here, as increasing the radiation parameter R thickens the fluid, reducing the temperature and thickness of the thermal boundary layer. As a result, raising the radiation parameter R causes the temperature to decrease across the fluid region. The Prandtl number describes the relationship between momentum diffusivity and thermal diffusivity, hence determining the relative thickness of the momentum and thermal boundary layers. Figure (11) shows that the temperature decreases as the Prandtl number Pr increases; also, the thickness of the thermal boundary layer is largest near the plate and decreases as one moves away from the leading edge, eventually approaching zero.

It is also justified by the fact that increasing the Prandtl number Pr reduces the fluid's thermal conductivity, resulting in a lower thermal boundary layer and temperature profile. Figure (12) demonstrates how increasing Schmidt number Sc results in lowering concentration patterns

Power System Technology
ISSN:1000-3673

Received: 1610-2024 Revised: 05-11-2024 Accepted: 22-12-2024

throughout the fluid.

Tables 1-3 provide the numerical values for skin friction (τ), Nusselt number (Nu), and Sherwood number (Sh). All of these tables compare each parameter to the first row of the related table. Table (1) indicates that raising R, D, Pr, Gr, Gm, Sc, and time t increases skin friction, while decreasing it with M and -Gr. Table (2) shows that when R, Pr, and t grow, so does the Nusselt number. Table (3) shows that the Sherwood number increases with increasing Sc and t.

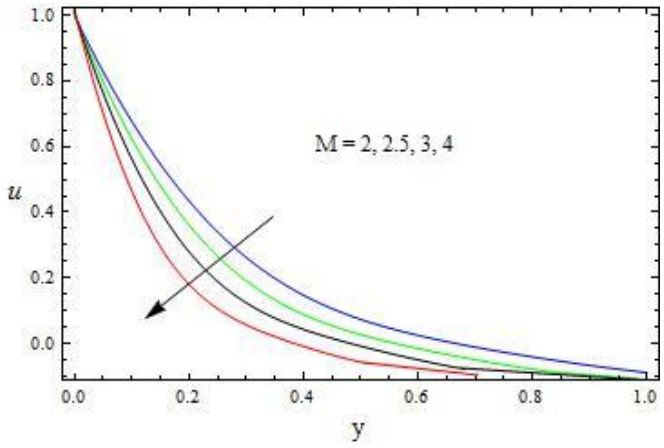

Fig 2.The velocity Profile for *u* against *M* with D=1; P= 0.71; t=0.1; Sc=2; R=1; Gr=5; Gm=10

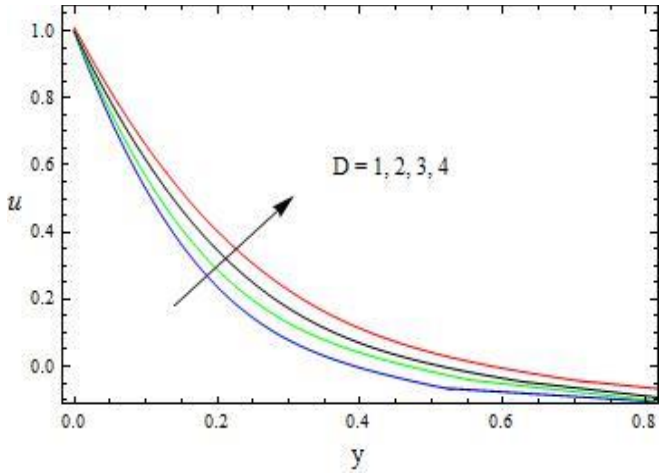

Fig 3. The velocity Profile for *u* against *D* with M=2; P= 0.71; t=0.1; Sc=2; R=1; Gr=5; Gm=10

Power System Technology
ISSN:1000-3673

Received: 1610-2024 Revised: 05-11-2024 Accepted: 22-12-2024

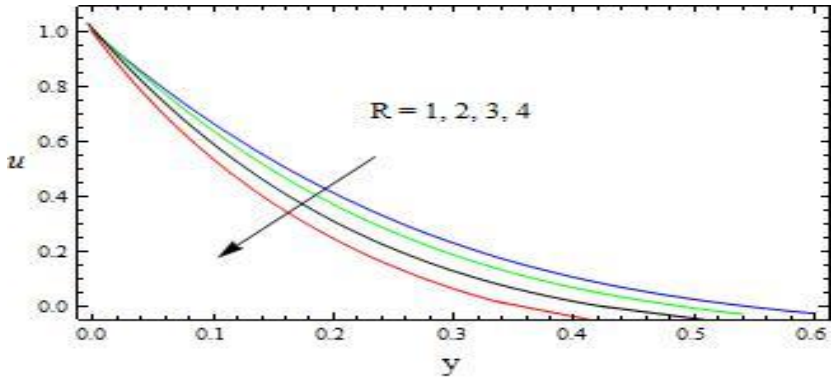

Fig 4. The velocity Profile for *u* against *R* with D=1; P= 0.71; t=0.1; Sc=2; M=2; Gr=5; Gm=10

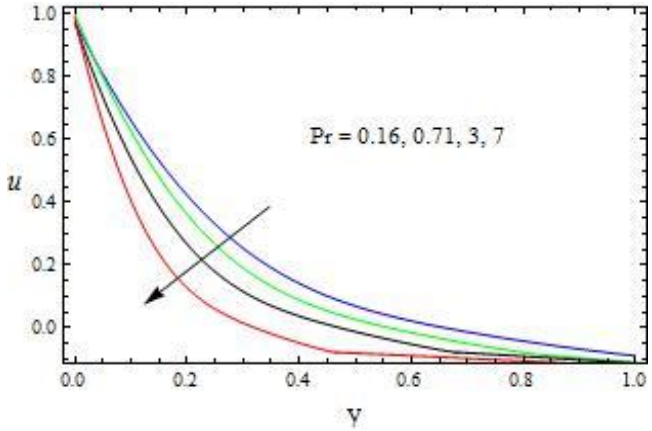

Fig 5. The velocity Profile for *u* against Pr and t with M=2; D=1; t=0.1; Sc=2; R=1; Gr=5; Gm=10

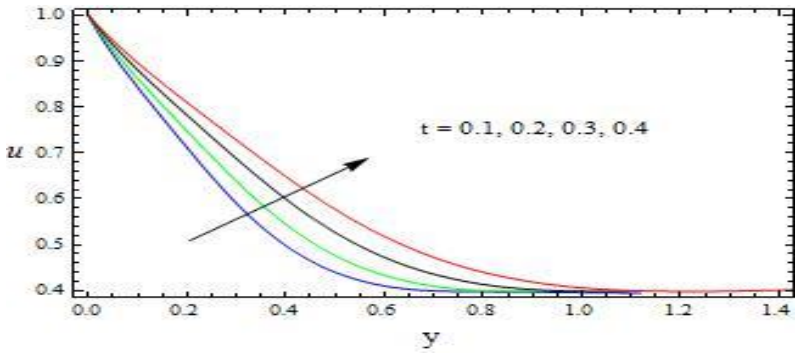

Fig 6. The velocity Profile for *u* against t with M=2; D=1; t=0.1; Sc=2; R=1; Gr=5; Gm=10

Power System Technology
ISSN:1000-3673

Received: 1610-2024 Revised: 05-11-2024 Accepted: 22-12-2024

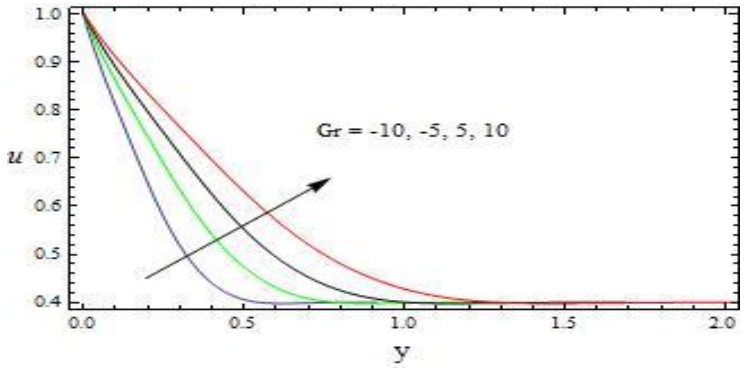

Fig 7. The velocity Profile for *u* against Gr with M=2; D=1; P=0.71, ; Sc=2; R=1; t=0.1; Gm=10

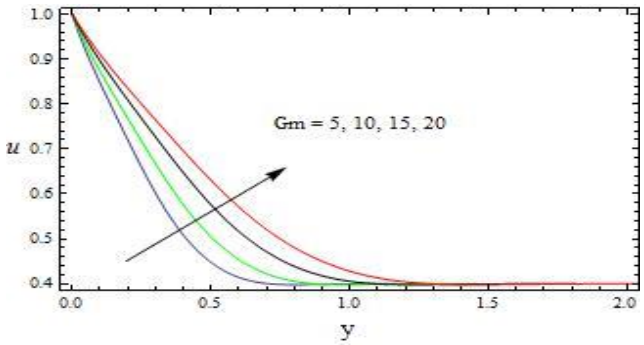

Fig 8. The velocity Profile for *u* against Gm with M=2; D=1; P=0.71, Sc=2; R=1; t=0.1; Gr=5

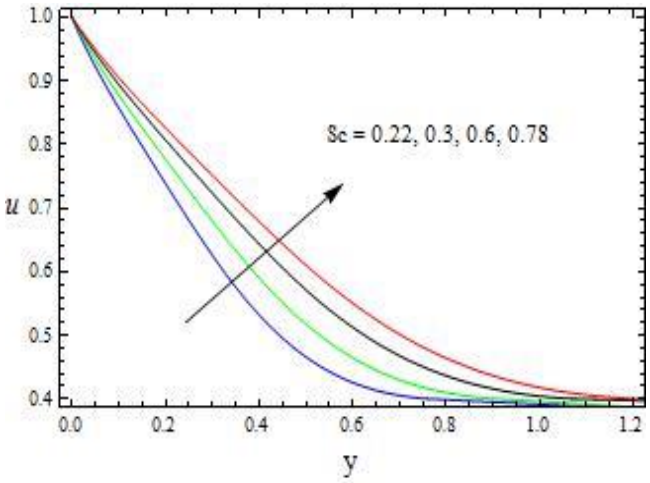

Fig 9. The velocity Profile for *u* against Sc with M=2; D=1; P=0.71, R=1; t=0.1; Gr=5; Gm=10

Power System Technology
ISSN:1000-3673

Received: 1610-2024 Revised: 05-11-2024 Accepted: 22-12-2024

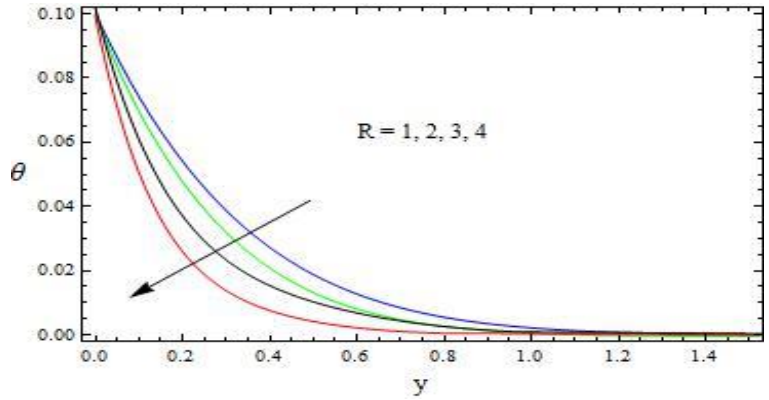

Fig 10. The Temperature Profile for θ against R with P=0.71; t=0.1

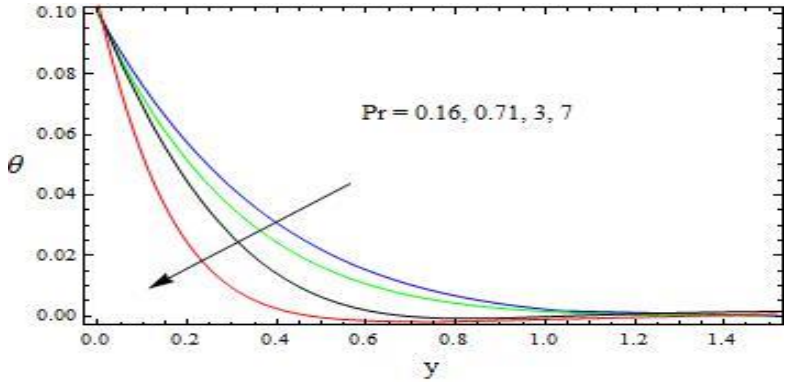

Fig 11. The Temperature Profile for θ against Pr with R=2; t=0.1

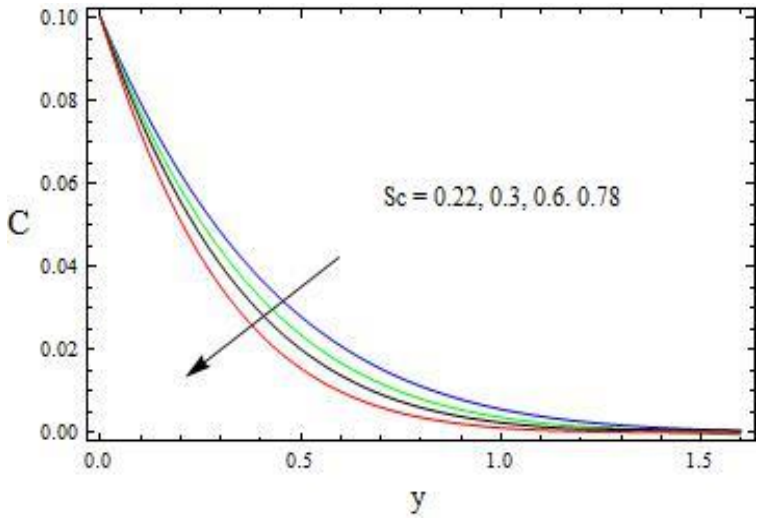

Fig 12. The Concentration Profile for C against Sc with t=0.1

Power System Technology
ISSN:1000-3673

Received: 1610-2024 Revised: 05-11-2024 Accepted: 22-12-2024

Table.1: The effects of various parameters on Skin friction (shear stress (τ))

R	M	D	Pr	Gr	Gm	Sc	t	τ
1	**2**	**1**	**0.71**	**5**	**10**	**2**	**0.2**	3.67042
2	2	1	0.71	5	10	2	0.2	4.29354
3	2	1	0.71	5	10	2	0.2	4.84244
1	**3**	1	0.71	5	10	2	0.2	3.48338
1	**4**	1	0.71	5	10	2	0.2	2.15628
1	2	**2**	0.71	5	10	2	0.2	3.70531
1	2	**3**	0.71	5	10	2	0.2	3.71552
1	2	1	**0.16**	5	10	2	0.2	3.14544
1	2	1	**3**	5	10	2	0.2	5.22357
1	2	1	**7**	5	10	2	0.2	10.4094
1	2	1	0.71	**10**	10	2	0.2	3.92357
1	2	1	0.71	**15**	10	2	0.2	4.17671
1	2	1	0.71	**-10**	10	2	0.2	2.91099
1	2	1	0.71	**-15**	10	2	0.2	2.65785
1	2	1	0.71	5	**5**	2	0.2	1.96178
1	2	1	0.71	5	**15**	2	0.2	5.37906
1	2	1	0.71	5	**20**	2	0.2	7.08770
1	2	1	0.71	5	10	**3**	0.2	3.78256
1	2	1	0.71	5	10	**4**	0.2	4.36933
1	2	1	0.71	5	10	**5**	0.2	4.99703
1	2	1	0.71	5	10	2	**0.3**	4.84466
1	2	1	0.71	5	10	2	**0.4**	6.06165
1	2	1	0.71	5	10	2	**0.5**	7.04960

Table.2: The effects of various parameters on the Rate of heat transfer (Nu)

R	Pr	t	Nu
1	**0.71**	**0.1**	0.195870
2	0.71	0.1	0.216376
3	0.71	0.1	0.235839
4	0.71	0.1	0.254358
1	**0.16**	0.1	0.107555
1	**3**	0.1	0.634710
1	**7**	0.1	1.393160

Power System Technology
ISSN:1000-3673

Received: 1610-2024 Revised: 05-11-2024 Accepted: 22-12-2024

1	0.71	**0.2**	0.331442
1	0.71	**0.3**	0.461249
1	0.71	**0.4**	0.588593

Table.3: The effects of various parameters on the Sherwood number (Sh)

Sc	t	Sh
2	**0.1**	0.104512
3	0.1	0.226218
4	0.1	0.356825
5	0.1	0.493120
2	**0.2**	0.147802
2	**0.3**	0.181019
2	**0.4**	0.209023
2	**0.5**	0.233695

4. . Conclusions

1. The velocity decreases as the Hartmann number, M, increases.
2. As the permeability parameter D values grow, so does the magnitude of the velocity. The magnitude of the velocity u increases and decreases constantly as the radiation parameter R increases.
3. The velocity increases as t increases. It is also noted that the magnitude of the velocity u decreases as the Prandtl number, Pr, increases.
4. The velocity falls as the thermal Grashof number Gr (cooling plate) increases, whereas there is a sudden increase in velocity for heating the plate, which continues away from it.
5. The magnitude of the velocity increases as the mass Grashof number Gm increases throughout the fluid region. The similar phenomena occur when the Schmidt number Sc increases.
6. The temperature decreases with increasing the radiation parameter R or Pr.
7. The increasing values of Schmidt number Sc lead to fall the concentration profiles throughout the fluid.
8. The skin friction enhances with increasing R, D, Pr, Gr, Gm, Sc and time *t*, while decreases with M and –Gr.
9. Nusselt number Nu increases with increasing R, Pr and *t*.
10. Sherwood number goes on increasing with increasing Sc and *t*.

Power System Technology
ISSN:1000-3673

Received: 1610-2024 Revised: 05-11-2024 Accepted: 22-12-2024

Sherwood number goes on increasing with increasing Sc and *t*.

References

1. O.D. Makinde, P.Y. Mhone, Heat transfer to MHD oscillatory flow in a channel filled with porous medium, Romanian J. Phys. 50 (2005) 931–938.
2. A. Mehmood, A. Ali, The effect of slip condition on unsteady MHD oscillatory flow of a viscous fluid in a planer channel, Romanian J. Phys. 52 (2007) 85–91.
3. D.S. Chauchan, V. Kumar, Radiation effects on mixed convection flow and viscous heating in a vertical channel partially filled with a porous medium, Tamkang J. Sci. Eng. 14 (2011) 97–106.
4. G. Palani, I.A. Abbas, Free convection MHD flow with thermal radiation from impulsively started vertical plate, Nonlinear Anal.: Model. Contr. 14 (2009) 73–84.
5. M. Hussain, T. Hayat, S. Asghar, C. Fetecau, Oscillatory flows of second grade fluid in a porous space, Nonlinear Anal.: Real World Appl. 11 (2010) 2403–2414.
6. J.C. Umavathi, A. J Chamkha, A. Mateenand, Al-Mudhat in a horizontal composite porous medium channel, Nonlinear Anal.: Model. Contr. 14 (2009) 397–415.
7. S.O. Adesanya, O.D. Makinde, Heat transfer to magnetohydrodynamic non-Newtonian couple stress pulsatile flow between two parallel porous plates, Z. Naturforsch. 67a (2012) 647–656.
8. O. Adesanya, J.A. Gbadeyan, Adomian decomposition approach to steady visco-elastic fluid flow with slip through a planer channel international, J. Nonlinear Sci. 9 (2010) 86–94.
9. S.O. Adesanya, E.O. Oluwadare, J.A. Falade, O.D. Makinde, Hydromagnetic natural convection flow between vertical parallel plates with time-periodic boundary conditions, J. Magn. Magn. Mater. 396 (2015) 295–303.
10. S.O. Adesanya, Free convective flow of heat generating fluid through a porous vertical channel with velocity slip and temperature jump, Ain Shams Eng. J. 6 (2015) 1045–1052.
11. S.O. Adesanya, J.A. Falade, O.D. Makinde, Pulsating flow through vertical porous channel with viscous dissipation effect, UPB. Sci. Bull. Ser. D 77 (1) (2015).
12. S.O. Adesanya, J.A. Falade, Thermodynamics analysis of hydromagnetic third grade fluid flow through a channel filled with porous medium, Alexandria Eng. J. 54 (2015)

Power System Technology
ISSN:1000-3673

Received: 1610-2024 Revised: 05-11-2024 Accepted: 22-12-2024

615–622.

13. J. Prakash, B.R. Kumar, R. Sivaraj, Radiation and Dufour effects on unsteady MHD mixed convective flow in an accelerated vertical wavy plate with varying temperature and mass diffusion, Walailak J. Sci. Technol. (WJST) 11 (11) (2014) 939–954.
14. R. Sivaraj, A. Jasmine Benazir, Unsteady magnetohydrodynamic mixed convective oscillatory flow of Casson fluid in a porous asymmetric wavy channel, Spec. Top. Rev. Porous Media: Int. J. 6 (3) (2015).
15. A. Jasmine Benazir, R. Sivaraj, O.D. Makinde, Unsteady magnetohydrodynamic Casson fluid flow over a vertical cone and flat plate with non-uniform heat source/sink, Int. J. Eng. Res. Afr. 21 (2016) 69–83.
16. A.J. Benazir, R. Sivaraj, M.M. Rashidi, Comparison between Casson fluid flow in the presence of heat and mass transfer from a vertical cone and flat plate, J. Heat Transfer 138 (11) (2016) 112005.
17. Seth GS, Sarkar S, Hussain SM. (2014), Effects of hall current, radiation and rotation on natural convection heat and mass transfer flow past a moving vertical plate. Ain Shams Engineering Journal 5: 489-503. http://doi.org/10.1016/j.asej.2013.09.014 [8] Biswas R, Mondal M, Sarkar DR, Ahmmed SF. (2017).
18. Biswas R, Mondal M, Sarkar DR, Ahmmed SF. (2017), Effects of radiation and chemical reaction on MHD unsteady heat and mass transfer of Casson fluid flow past a vertical plate. Journal of Advances in Mathematics and Computer Science, 23(2), 1-16. http://doi.org/10.9734/JAMCS/2017/34292
19. S.F. Ahmmed, R. Biswas, Effects of radiation and chemical reaction on MHD unsteady heat and mass transfer of nanofluid flow through a vertical plate, Vol. 87, No. 4, December, 2018, pp. 213-220, https://doi.org/10.18280/mmc_b.870401
20. Chamkha AJ, Khaled AR. Similarity solutions for hydromagnetic simultaneous heat and mass transfer. Heat and Mass Transfer 2001; 37:117–123.
21. T. Hayat and Z. Abbas, Effects of radiation and magnetic field on the mixed convection stagnation-point flow over a vertical stretching sheet in a porous medium, International Journal of Heat and Mass Transfer 53 (2010) 466–474
22. Sweta Matta, Bala Siddulu Malga and Lakshmi Appidi1, Radiation and chemical reaction effects on unsteady MHD free convention mass transfer fluid flow in a porous plate, Indian Journal of Science and Technology 2021,14(8):707–717, ISSN: 0974-6846